Frontiers of Information Technology & Electronic Engineering
www.jzus.zju.edu.cn; engineering.cae.cn; www.springerlink.com
ISSN 2095-9184 (print); ISSN 2095-9230 (online)
E-mail: jzus@zju.edu.cn

Asynchronous gain-scheduled control of deepwater drilling riser system with hybrid event-triggered sampling and unreliable communication*#

Na PANG, Dawei ZHANG, Shuqian ZHU†‡

School of Mathematics, Shandong University, Jinan 250100, China

†E-mail: sqzhu@sdu.edu.cn

Received Sept. 14, 2023; Revision accepted Dec. 10, 2023; Crosschecked Dec. 18, 2023; Published online Dec. 29, 2023

Abstract: This paper investigates the recoil control of the deepwater drilling riser system with nonlinear tension force and energy-bounded friction force under the circumstances of limited network resources and unreliable communication. Different from the existing linearization modeling method, a triangle-based polytope modeling method is applied to the nonlinear riser system. Based on the polytope model, to improve resource utilization and accommodate random data loss and communication delay, an asynchronous gain-scheduled control strategy under a hybrid event-triggered scheme is proposed. An asynchronous linear parameter-varying system that blends input delay and impulsive update equation is presented to model the nonlinear networked recoil control system, where the asynchronous deviation bounds of scheduling parameters are calculated. Resorting to the Lyapunov–Krasovskii functional method, some solvable conditions of disturbance attenuation analysis and recoil control design are derived such that the resulting networked system is exponentially mean-square stable with prescribed H_∞ performance. The obtained numerical results verified that the proposed nonlinear networked control method can achieve a better recoil response of the riser system with less transmission data compared with the linear control method.

Key words: Riser system; Recoil control; Asynchronous gain-scheduled control; Data loss; Event-triggered scheme
https://doi.org/10.1631/FITEE.2300625 **CLC number:** TP13

1 Introduction

The deepwater drilling riser system is a class of key marine engineering equipment that connects offshore drilling platforms and underwater wellhead systems during drilling operations. To ensure the safety of equipment and platform staff when facing the extremely harsh ocean environment or the failure of dynamic positioning systems, the riser system is required to implement the emergency disconnection between the lower marine riser package and the subsea blowout preventer. In this situation, the riser quickly recoils upwards, and this recoil, caused by elastic potential energy and friction resistance of drilling fluid, is named the recoil response (Liu XQ et al., 2022; Wang XL et al., 2022). If the recoil response is not properly suppressed, the platform staff and the riser equipment are in great danger.

In the past decade, considerable effort has been put into addressing the recoil response suppression of riser systems (Pestana et al., 2016; Liu J et al., 2018; Wang T and Liu, 2018; Liu XQ et al., 2021; Wang XL et al., 2021, 2022). In the prevalent

‡ Corresponding author
* Project supported by the National Natural Science Foundation of China (Nos. 62373220 and 62173209) and the Shandong Provincial Natural Science Foundation of China (No. ZR2023MF011)
# Electronic supplementary materials: The online version of this article (https://doi.org/10.1631/FITEE.2300625) contains supplementary materials, which are available to authorized users
ORCID: Shuqian ZHU, https://orcid.org/0000-0002-2560-1465

literature dealing with the topic, the main challenging problems pertain to the means of characterizing the coupled dynamics model of the recoil control process and that of designing the efficient control strategies for satisfactory response suppression. In Liu XQ et al. (2020, 2021), Meng et al. (2020), and Zhao et al. (2022a, 2022b), using the finite element method and the concentrated mass method, a linear spring-mass-damping model was used for axial dynamic analysis of risers. With such a linear model, to suppress the effect of friction force on recoil response, Zhao et al. (2022a) designed a pure delayed H_∞ controller (PDHC), Zhao et al. (2022b) designed an optimal recoil controller with feedforward compensation, Zhang W et al. (2023a) proposed an observer-based dynamic output-feedback controller, and Zhang W et al. (2023b) proposed a delayed state-feedback H_∞ controller. In fact, the tension force produced by the tensioner is essentially nonlinear (Pestana et al., 2016; Wang T and Liu, 2018; Liu XQ et al., 2021). Although the linearization method based on the Taylor expansion is commonly used to model the riser-tensioner system (Zhao et al., 2022a, 2022b; Zhang W et al., 2023a, 2023b), it unavoidably causes an unsatisfactory control performance by the linear recoil control strategies when linearization errors are ignored. Thus, it is particularly necessary to present some specialized nonlinear modeling and recoil control methods for the riser-tensioner system.

Notice that the existing recoil control strategies so far have been designed in a traditional control system structure. From the perspective of modern industrial control, the prevalent networking technology and networked control system (NCS) structure can bring revolutionary progress and attractive advantages such as remote control and diagnostics, flexible system layout, and low implementation cost (Ma et al., 2019; Zhang XM et al., 2020; Shi et al., 2021). Since offshore drilling platforms tend to operate in a deep-sea field to explore more oil or gas resources, the operational environment of the drilling riser system poses some significant challenges to stability and safety (Dinh et al., 2017; He et al., 2020; Liu Y et al., 2022). Currently, the satellite communication network and other dedicated wireless ad-hoc networks are used mainly to deploy the network environment of marine engineering equipment in a deep-sea environment. Such types of networks are with limited resources and relatively low reliability, and they can impose imperfect constraints such as communication delay and random data loss, which further affect the control performance (Zou et al., 2016; Hu et al., 2020; Zhang DW et al., 2020; Zhang XM et al., 2022, 2023). Accordingly, it is necessary to develop some networked nonlinear modeling and recoil control methods of riser-tensioner systems that can be deployed under the circumstances of limited network resources and unreliable communication (Coutinho and Palhares, 2021; Zhang BL et al., 2021).

This paper proposes several networked recoil control system modeling and asynchronous gain-scheduled control methods for riser-tensioner systems subject to limited network resources, unavoidable communication delay, and unreliable communication. Since the nonlinear riser-tensioner system in the existing forms depends on the displacement of the first mass block that is physically measurable, an equivalent form of the nonlinear riser-tensioner system is reformulated by a triangle-based polytope model inspired by the nonlinear modeling advantage of linear parameter-varying (LPV) systems (Li WF et al., 2020; Chu et al., 2022). To save network resources and against the random data loss, the hybrid event-triggered sampling scheme in Gao et al. (2023) is introduced to collect the necessary displacement and velocity information of the riser-tensioner system. Considering that the LPV model with the schedulable displacement information and the transmitted information is affected by the communication delay and the possible data loss, an asynchronous gain-scheduled control scheme is presented to implement the networked control. The resulting nonlinear NCS of the riser-tensioner system is modeled by an asynchronous parameter-scheduled system with sampling and random impulsive updates. For such a system, a computation method of the asynchronous deviation bounds of the scheduling parameters is provided and a discontinuous Lyapunov–Krasovskii functional method is applied to derive an H_∞ performance analysis criterion. Using the deviation bounds and the analysis results, a nonlinear design of the asynchronous gain-scheduled controller (AGSC) is developed. Finally, the NCS modeling and recoil control methods of the riser-tensioner system are numerically verified.

The main contributions of the present research are summarized below:

1. A specialized nonlinear NCS modeling

method of the riser-tensioner system subject to event-triggered scheme, communication delay, and random data loss is proposed by applying the LPV system approach and the hybrid sampled-data system and impulsive system approach.

2. An asynchronous gain-scheduled control strategy is presented to suppress the recoil response of the networked riser-tensioner system with friction force as much as possible in the H_∞ control sense.

3. A case study is carried out, which reveals that the proposed nonlinear networked recoil control method, compared with the common linear control method, can achieve a better control effect and suppression performance in the network environment, and can save network resources with the event-triggered scheme.

2 Nonlinear networked control system modeling and recoil control of the riser-tensioner system

2.1 Triangle-based polytope linear parameter-varying model of the riser-tensioner system

Usually, the deepwater drilling riser-tensioner system is simplified as a spring-mass-damping model with three degrees of freedom (Wang YB and Gao, 2019; Liu XQ et al., 2021; Zhao et al., 2022a, 2022b), and the dynamic equations of the model are given by

$$\begin{cases} m_1\ddot{x}_1(t) = F(t) - c_1\dot{x}_1(t) - m_1g + F_{\mathrm{b}_1} \\ \qquad\qquad -k_2(x_1(t)-x_2(t)) - F_{\mathrm{w}_1}(t) \\ \qquad\qquad -c_2(\dot{x}_1(t)-\dot{x}_2(t)) - F_{\mathrm{m}_1}(t), \\ m_2\ddot{x}_2(t) = k_2(x_1(t)-x_2(t)) + c_2(\dot{x}_1(t)-\dot{x}_2(t)) \\ \qquad\qquad -m_2g - k_3(x_2(t)-x_3(t)+x_0) + F_{\mathrm{b}_2} \\ \qquad\qquad -c_3(\dot{x}_2(t)-\dot{x}_3(t)) - F_{\mathrm{w}_2}(t) - F_{\mathrm{m}_2}(t), \\ m_3\ddot{x}_3(t) = k_3(x_2(t)-x_3(t)+x_0) - m_3g + F_{\mathrm{b}_3} \\ \qquad\qquad +c_3(\dot{x}_2(t)-\dot{x}_3(t)) - F_{\mathrm{w}_3}(t) - F_{\mathrm{m}_3}(t), \end{cases} \tag{1}$$

with the following model of the tension force $F(t)$ (Liu XQ et al., 2021):

$$F(t) = \frac{P_{\mathrm{H}_0}V_{\mathrm{H}_0}^{\kappa}A_{\mathrm{r}}}{(V_{\mathrm{H}_0}+A_{\mathrm{r}}x_1(t))^{\kappa}} - \frac{P_{\mathrm{L}_0}V_{\mathrm{L}_0}^{\kappa}A_{\mathrm{p}}}{(V_{\mathrm{L}_0}-A_{\mathrm{p}}x_1(t))^{\kappa}} - u(t). \tag{2}$$

Here, $x_0 = (P_{\mathrm{H}_0}A_{\mathrm{r}} - P_{\mathrm{L}_0}A_{\mathrm{p}} - m_1g + F_{\mathrm{b}_1})/k_2$; m_i's $(i=1,2,3)$ represent three equivalent mass blocks; c_i $(i=1,2,3)$ is the damping coefficient; $x_i(t)$ $(i=1,2,3)$ is the displacement at time t; k_i $(i=2,3)$ is the stiffness; g is the acceleration of gravity; $F_{\mathrm{w}_i}(t)$ and $F_{\mathrm{m}_i}(t)$ $(i=1,2,3)$ are the friction forces of seawater and drilling mud discharge, respectively; F_{b_i}'s $(i=1,2,3)$ denote the axial buoyancy of three mass blocks; P_{H_0} and P_{L_0} are the pressures of the high- and low-pressure gas at the initial moment, respectively; V_{H_0} and V_{L_0} are the volumes of the high- and low-pressure gas at the initial moment, respectively; A_{r} and A_{p} are the areas of piston at the rod and rod-less sides, respectively; κ is a constant relative to the properties of gas and it is generally assumed to be $\kappa=1$; $u(t)$ is the pressure drop generated by the recoil control.

Clearly, $F(t)$ is nonlinear with respect to $x_1(t)$, which results in the riser-tensioner system (1) being a nonlinear system. Usually, a linearization method based on the Taylor expansion is adopted to convert system (1) to a linear system with the sacrifice of approximation accuracy (Zhao et al., 2022a, 2022b; Zhang W et al., 2023a, 2023b). To better model the nonlinearity, the LPV system modeling method is proposed as follows. Let

$$\tilde{z}(t) = [\tilde{z}_1(t) \quad \tilde{z}_2(t) \quad \tilde{z}_3(t) \quad \tilde{z}_4(t) \quad \tilde{z}_5(t) \quad \tilde{z}_6(t)]^{\mathrm{T}}$$

with

$$\begin{cases} \tilde{z}_1(t) = x_1(t), \quad \tilde{z}_2(t) = \dot{x}_1(t), \quad \tilde{z}_3(t) = x_2(t), \\ \tilde{z}_4(t) = \dot{x}_2(t), \quad \tilde{z}_5(t) = x_3(t), \quad \tilde{z}_6(t) = \dot{x}_3(t). \end{cases}$$

Using Eq. (1), the initial displacement values at the moment of emergency disconnection are given by

$$\begin{cases} \tilde{z}_1(0) = 0, \\ \tilde{z}_3(0) = -x_0, \\ \tilde{z}_5(0) = -(k_2x_0 - m_2g + F_{\mathrm{b}_2})/k_3, \end{cases}$$

and the equilibrium point is computed by

$$\bar{z}_0 = [\bar{z}_{01} \quad \bar{z}_{02} \quad \bar{z}_{03} \quad \bar{z}_{04} \quad \bar{z}_{05} \quad \bar{z}_{06}]^{\mathrm{T}},$$

where

$$\begin{cases} \bar{z}_{02} = \bar{z}_{04} = \bar{z}_{06} = 0, \\ \dfrac{P_{\mathrm{H}_0}V_{\mathrm{H}_0}A_{\mathrm{r}}}{V_{\mathrm{H}_0}+A_{\mathrm{r}}\bar{z}_{01}} - \dfrac{P_{\mathrm{L}_0}V_{\mathrm{L}_0}A_{\mathrm{p}}}{V_{\mathrm{L}_0}-A_{\mathrm{p}}\bar{z}_{01}} - m_1g \\ -m_2g - m_3g + F_{\mathrm{b}_1} + F_{\mathrm{b}_2} + F_{\mathrm{b}_3} = 0, \\ \bar{z}_{03} = \bar{z}_{01} + (-m_2g - m_3g + F_{\mathrm{b}_2} + F_{\mathrm{b}_3})/k_2, \\ \bar{z}_{05} = \bar{z}_{03} + x_0 + (-m_3g + F_{\mathrm{b}_3})/k_3. \end{cases}$$

Let $z(t) = \tilde{z}(t) - \bar{z}_0$. One can obtain the LPV system form of the riser-tensioner system (1) as follows:

$$\dot{z}(t) = A(z_1(t))z(t) + Bu(t) + \bar{D}\theta_1(t), \tag{3}$$

where

$$A(z_1(t))=\begin{bmatrix} A_{11}(z_1(t)) & A_{12} \\ A_{21} & A_{22} \end{bmatrix},$$

$$A_{11}(z_1(t))=\begin{bmatrix} 0 & 1 \\ -\dfrac{k_2}{m_1}+\dfrac{\Upsilon(z_1(t))}{z_1(t)} & -\dfrac{c_1+c_2}{m_1} \end{bmatrix},$$

$$A_{12}=\begin{bmatrix} 0 & 0 & 0 & 0 \\ \dfrac{k_2}{m_1} & \dfrac{c_2}{m_1} & 0 & 0 \end{bmatrix},$$

$$A_{21}=\begin{bmatrix} 0 & \dfrac{k_2}{m_2} & 0 & 0 \\ 0 & \dfrac{c_2}{m_2} & 0 & 0 \end{bmatrix}^{\mathrm{T}},$$

$$A_{22}=\begin{bmatrix} 0 & 1 & 0 & 0 \\ -\dfrac{k_2+k_3}{m_2} & -\dfrac{c_2+c_3}{m_2} & \dfrac{k_3}{m_2} & \dfrac{c_3}{m_2} \\ 0 & 0 & 0 & 1 \\ \dfrac{k_3}{m_3} & \dfrac{c_3}{m_3} & -\dfrac{k_3}{m_3} & -\dfrac{c_3}{m_3} \end{bmatrix},$$

$$B=\begin{bmatrix} 0 & -\dfrac{1}{m_1} & 0 & 0 & 0 & 0 \end{bmatrix}^{\mathrm{T}},$$

$$\bar{D}=\begin{bmatrix} 0 & -\dfrac{1}{m_1} & 0 & 0 & 0 & 0 \\ 0 & 0 & 0 & -\dfrac{1}{m_2} & 0 & 0 \\ 0 & 0 & 0 & 0 & 0 & -\dfrac{1}{m_3} \end{bmatrix}^{\mathrm{T}},$$

$$\theta_1(t)=\begin{bmatrix} F_{\mathrm{w}_1}(t)+F_{\mathrm{m}_1}(t) \\ F_{\mathrm{w}_2}(t)+F_{\mathrm{m}_2}(t) \\ F_{\mathrm{w}_3}(t)+F_{\mathrm{m}_3}(t) \end{bmatrix},$$

$$\begin{aligned}\Upsilon(z_1(t))=&\frac{P_{\mathrm{H}_0}V_{\mathrm{H}_0}A_{\mathrm{r}}}{m_1(V_{\mathrm{H}_0}+A_{\mathrm{r}}(z_1(t)+\bar{z}_{01}))}\\ &-\frac{P_{\mathrm{L}_0}V_{\mathrm{L}_0}A_{\mathrm{p}}}{m_1(V_{\mathrm{L}_0}-A_{\mathrm{p}}(z_1(t)+\bar{z}_{01}))}\\ &-\frac{P_{\mathrm{H}_0}V_{\mathrm{H}_0}A_{\mathrm{r}}}{m_1(V_{\mathrm{H}_0}+A_{\mathrm{r}}\bar{z}_{01})}+\frac{P_{\mathrm{L}_0}V_{\mathrm{L}_0}A_{\mathrm{p}}}{m_1(V_{\mathrm{L}_0}-A_{\mathrm{p}}\bar{z}_{01})}.\end{aligned}$$

The initial state of system (3) is denoted as $z(0)=z_0$. By solving the external force $h(t)$ in a manner similar to that was adopted in Li CW et al. (2016) and Zhao et al. (2022a, 2022b), one further obtains the riser-tensioner system:

$$\dot{z}(t)=A(z_1(t))z(t)+Bu(t)+Dh(t), \tag{4}$$

where

$$\begin{aligned}&h(t)=(F_{\mathrm{w}}(t)+F_{\mathrm{m}}(t))/3,\\ &F_{\mathrm{w}}(t)=3F_{\mathrm{w}_i}(t),\ i=1,2,3,\\ &F_{\mathrm{m}}(t)=3F_{\mathrm{m}_i}(t),\ i=1,2,3,\\ &F_{\mathrm{w}_i}(t)=\frac{\rho_{\mathrm{w}}v^2(t)f_{\mathrm{w}}A_{\mathrm{s}}L_{\mathrm{w}}(t)}{6D_{\mathrm{e}}},\ i=1,2,3,\\ &F_{\mathrm{m}_i}(t)=\frac{\rho_{\mathrm{m}}v^2(t)f_{\mathrm{m}}A_{\mathrm{s}}(L_{\mathrm{r}}-L_{\mathrm{w}}(t))}{6D_{\mathrm{e}}},\ i=1,2,3,\\ &v(t)=v(t-\Delta t)+a(t)\Delta t,\\ &b(t)=0.5a(t)(\Delta t)^2,\\ &L_{\mathrm{w}}(t)=L_{\mathrm{w}}(t-\Delta t)+v(t-\Delta t)\Delta t+b(t),\\ &a(t)=\frac{\mathcal{F}(t)-3F_{\mathrm{w}_i}(t)-3F_{\mathrm{m}_i}(t)-0.5\rho_{\mathrm{m}}A_{\mathrm{s}}v^2(t)}{\rho_{\mathrm{m}}A_{\mathrm{s}}(L_{\mathrm{r}}-L_{\mathrm{w}}(t))+\rho_{\mathrm{w}}A_{\mathrm{s}}L_{\mathrm{w}}(t)},\\ &\mathcal{F}(t)=(L_{\mathrm{r}}-L_{\mathrm{w}}(t))(\rho_{\mathrm{m}}-\rho_{\mathrm{w}})gA_{\mathrm{s}},\\ &D=\begin{bmatrix} 0 & -\dfrac{1}{\mathrm{m}_1} & 0 & -\dfrac{1}{\mathrm{m}_2} & 0 & -\dfrac{1}{\mathrm{m}_3} \end{bmatrix}^{\mathrm{T}}.\end{aligned}$$

Here, $F_{\mathrm{w}}(t)$ and $F_{\mathrm{m}}(t)$ are the friction forces of seawater and drilling mud discharge, respectively; ρ_{w} and ρ_{m} are the densities of seawater and drilling mud discharge, respectively; f_{w} and f_{m} are the friction coefficients of seawater and drilling mud discharge, respectively; $L_{\mathrm{w}}(t)$ and L_{r} are the length of seawater section at time t and the length of the riser, respectively; $v(t)$ is the discharge velocity at time t; Δt is the time increment; $a(t)$ is the average acceleration in each time step from $t-\Delta t$ to t; A_{s} is the hydraulic area of the riser; D_{e} is the diameter of the riser.

Note that $A(z_1(t))$ is a time-varying nonlinear matrix with respect to bounded $z_1(t)$. Inspired by Gao et al. (2022), a triangle-based polytope modeling method is introduced by designing the scheduling variables. The specific modeling process is stated as follows:

(1) Determine the nonlinear parameter set $\left\{\dfrac{1}{q_1(t)},\dfrac{1}{q_2(t)}\right\}$ in $A(z_1(t))$ by

$$\begin{cases} \dfrac{1}{q_1(t)}=\dfrac{1}{z_1(t)+(V_{\mathrm{H}_0}+A_{\mathrm{r}}\bar{z}_{01})/A_{\mathrm{r}}}, \\ \dfrac{1}{q_2(t)}=\dfrac{1}{z_1(t)+(A_{\mathrm{p}}\bar{z}_{01}-V_{\mathrm{L}_0})/A_{\mathrm{p}}}. \end{cases}$$

(2) Compute the range of the set $\left\{\dfrac{1}{q_1(t)},\dfrac{1}{q_2(t)}\right\}$ for given $z_1(t)\in[\underline{z}_1,\overline{z}_1]$, which can be denoted by $\dfrac{1}{q_1(t)}\in\left[\dfrac{1}{\overline{q}_1},\dfrac{1}{\underline{q}_1}\right]$ and $\dfrac{1}{q_2(t)}\in\left[\dfrac{1}{\overline{q}_2},\dfrac{1}{\underline{q}_2}\right]$.

(3) Use a triangle polytope composed of three vertices $D_1\triangleq\left(\dfrac{1}{\underline{q}_1},\dfrac{1}{\underline{q}_2}\right)$, $D_2\triangleq\left(\dfrac{1}{\underline{q}_1},\dfrac{1}{\overline{q}_2}\right)$, $D_3\triangleq\left(\dfrac{1}{\overline{q}_1},\dfrac{1}{\overline{q}_2}\right)$ to wrap the curve shaped by

$\left\{\dfrac{1}{q_1(t)}, \dfrac{1}{q_2(t)}\right\}$ and then present the polytope LPV model of system (4) as follows:

$$\dot{z}(t)=\sum_{i=1}^{3}\varsigma_i(t)A_iz(t)+Bu(t)+Dh(t), \tag{5}$$

where the scheduling parameter $\varsigma_i(t)$ $(i=1,2,3)$ and the coefficient matrix A_i $(i=1,2,3)$ can be obtained using the following lemma:

Lemma 1 Define the following notations:

$$\overline{v}_1(z_1(t))=\left(\frac{1}{q_1(t)}-\frac{1}{\overline{q}_1}\right)\Big/\left(\frac{1}{\underline{q}_1}-\frac{1}{\overline{q}_1}\right),$$

$$\overline{v}_2(z_1(t))=\left(\frac{1}{q_2(t)}-\frac{1}{\overline{q}_2}\right)\Big/\left(\frac{1}{\underline{q}_2}-\frac{1}{\overline{q}_2}\right),$$

$$\underline{v}_1(z_1(t))=\left(\frac{1}{\underline{q}_1}-\frac{1}{q_1(t)}\right)\Big/\left(\frac{1}{\underline{q}_1}-\frac{1}{\overline{q}_1}\right),$$

$$\underline{v}_2(z_1(t))=\left(\frac{1}{\underline{q}_2}-\frac{1}{q_2(t)}\right)\Big/\left(\frac{1}{\underline{q}_2}-\frac{1}{\overline{q}_2}\right).$$

Then the parameters and matrices in system (5) can be computed by

$$\varsigma_1(t)=\overline{v}_2(z_1(t)),$$
$$\varsigma_2(t)=\overline{v}_1(z_1(t))-\overline{v}_2(z_1(t)),$$
$$\varsigma_3(t)=\underline{v}_1(z_1(t)),$$
$$A_i=\begin{bmatrix}A_{i_{11}} & A_{12}\\ A_{21} & A_{22}\end{bmatrix},\ i=1,2,3,$$
$$A_{i_{11}}=\begin{bmatrix}0 & 1\\ -\dfrac{k_2}{m_1}+\Upsilon_i & -\dfrac{c_1+c_2}{m_1}\end{bmatrix},\ i=1,2,3,$$
$$\Upsilon_1=-\frac{P_{\mathrm{H}_0}V_{\mathrm{H}_0}A_{\mathrm{r}}}{m_1(V_{\mathrm{H}_0}+A_{\mathrm{r}}\bar{z}_{01})}\frac{1}{\underline{z}_1+(V_{\mathrm{H}_0}+A_{\mathrm{r}}\bar{z}_{01})/A_{\mathrm{r}}}+\frac{P_{\mathrm{L}_0}V_{\mathrm{L}_0}A_{\mathrm{p}}}{m_1(V_{\mathrm{L}_0}-A_{\mathrm{p}}\bar{z}_{01})}\frac{1}{\underline{z}_1+(A_{\mathrm{p}}\bar{z}_{01}-V_{\mathrm{L}_0})/A_{\mathrm{p}}},$$
$$\Upsilon_2=-\frac{P_{\mathrm{H}_0}V_{\mathrm{H}_0}A_{\mathrm{r}}}{m_1(V_{\mathrm{H}_0}+A_{\mathrm{r}}\bar{z}_{01})}\frac{1}{\underline{z}_1+(V_{\mathrm{H}_0}+A_{\mathrm{r}}\bar{z}_{01})/A_{\mathrm{r}}}+\frac{P_{\mathrm{L}_0}V_{\mathrm{L}_0}A_{\mathrm{p}}}{m_1(V_{\mathrm{L}_0}-A_{\mathrm{p}}\bar{z}_{01})}\frac{1}{\overline{z}_1+(A_{\mathrm{p}}\bar{z}_{01}-V_{\mathrm{L}_0})/A_{\mathrm{p}}},$$
$$\Upsilon_3=-\frac{P_{\mathrm{H}_0}V_{\mathrm{H}_0}A_{\mathrm{r}}}{m_1(V_{\mathrm{H}_0}+A_{\mathrm{r}}\bar{z}_{01})}\frac{1}{\overline{z}_1+(V_{\mathrm{H}_0}+A_{\mathrm{r}}\bar{z}_{01})/A_{\mathrm{r}}}+\frac{P_{\mathrm{L}_0}V_{\mathrm{L}_0}A_{\mathrm{p}}}{m_1(V_{\mathrm{L}_0}-A_{\mathrm{p}}\bar{z}_{01})}\frac{1}{\overline{z}_1+(A_{\mathrm{p}}\bar{z}_{01}-V_{\mathrm{L}_0})/A_{\mathrm{p}}}.$$

2.2 Networked asynchronous gain-scheduled control formulation

For the LPV system (5), the following controller is proposed:

$$u(t)=\sum_{i=1}^{3}\varsigma_i(t)K_iz(t), \tag{6}$$

where K_i $(i=1,2,3)$ is the control gain to be designed. To save communication resources and tolerate the random data loss (Ge et al., 2019, 2020, 2021, 2022; Jiang et al., 2021; Sun et al., 2021; Wei et al., 2021; Liu ZQ et al., 2022), the hybrid event-triggered sampling scheme in Gao et al. (2023) is introduced as follows:

$$\begin{cases}t_{k+1}h=t_kh+\min\{\varkappa,h_k\},\\ h_k=\min\limits_{i\in\mathbb{N}}\{ih\mid\!\mid\!\mid (z(t_kh)-z((t_k+i)h))^{\mathrm{T}}T^{\frac{1}{2}}\mid\!\mid\\ \qquad >\sigma\mid\!\mid z^{\mathrm{T}}(t_kh)T^{\frac{1}{2}}\mid\!\mid\},\end{cases} \tag{7}$$

where h is the sampling period, $\sigma>0$ is the threshold coefficient, $T>0$ is the weighting matrix, $\varkappa$ is the fixed triggering size, and $\mathbb{N}$ is the set of natural numbers. As shown in Gao et al. (2023), the main advantages of the event-triggered scheme (7) lie at solving the problem of random data loss of triggered data, providing a balanced choice between the fixed triggering size and the data loss probability, and improving the transient and steady performance. In scheme (7), T can be co-designed with the control design result, and the parameters $\varkappa$ and σ are pre-set. As $\varkappa$ is inversely proportional to the maximum allowable data loss probability, one can set the value of $\varkappa$ according to rental network protocols. σ can be freely adjusted to satisfy $0<\sigma<1$, meeting the expected transmission efficiency. Notice that the scheduling parameter $\varsigma_i(t)$ $(i=1,2,3)$ in controller (6) is the function of the displacement information $z_1(t)$ to be sampled and transmitted. Since the triggered scheme (7) is introduced, the data $\varsigma_i(t_kh)$ are available for control computing. Due to the effect of inevitable communication delay τ_{t_k} and possible random data loss, the scheduling parameters cannot be shared synchronously between the system and the controller. Thus, the control input is constructed as follows:

$$u(t)=\sum_{i=1}^{3}\varsigma_i(t_kh)K_i\hat{z}(t_kh)$$

$$=\sum_{i=1}^{3}\varsigma_i(t_kh)K_iz(t_kh)+(1-\beta_k)\cdot\sum_{i=1}^{3}\varsigma_i(t_kh)K_i(\hat{z}(t_{k-1}h)-z(t_kh)) \tag{8}$$

for $t\in\{t_kh+\tau_{t_k}\}_{k\in\mathbb{N}}$, where $\hat{z}(t_kh)=\beta_kz(t_kh)+(1-\beta_k)\hat{z}(t_{k-1}h)$ $(\forall k\in\mathbb{N})$, $\hat{z}(t_{-1}h)=0$ is set to compute the triggered data $\hat{z}(t_0h)$, and β_k is a stochastic variable obeying the Bernoulli distribution with the probabilities $\text{Prob}\{\beta_k=1\}=\beta$ and $\text{Prob}\{\beta_k=0\}=1-\beta$ with $\beta\in(0,1]$. Using the input delay method, one can transform the control input (8) into

$$u(t)=\sum_{i=1}^{3}\varsigma_i(t-\tau(t))K_i(z(t-\tau(t))-\nu_k(t-\tau(t)))+\sum_{i=1}^{3}\varsigma_i(t-\tau(t))K_i(1-\beta_k)d(t), \tag{9}$$

where $\tau(t)=t-(t_k+i)h$, $t\in\mathcal{F}_{k,i}$ $(i=0,1,\ldots,\mathcal{J}_k,\forall k\in\mathbb{N})$, $\mathcal{F}_{k,i}=[f_{t_k+i},f_{t_k+i+1})$, $f_{t_k+i}=(t_k+i)h+\tau_{t_k+i}$, $\mathcal{J}_k=t_{k+1}-t_k-1$, $\nu_k(t-\tau(t))=z(t-\tau(t))-z(t_kh)$, and $d(t)=\hat{z}(t_{k-1}h)-z(t_kh)$. Clearly, $\bigcup_{i=0}^{\mathcal{J}_k}\mathcal{F}_{k,i}=[f_{t_k},f_{t_{k+1}})$ and $0\le\tau_{t_k+i}\le\tau(t)\le\tau_{t_k+i+1}+h\le\eta_M=\sup_{k\in\mathbb{N}}\{\tau_{t_k+i}+h\}$, which implies that the allowable upper bound of communication delay is $\tau_M=\sup_{k\in\mathbb{N}}\{\tau_{t_k+i}\}=\eta_M-h$.

2.3 Networked riser-tensioner system and recoil control problem statement

Substituting the control input (9) into system (5), the networked riser-tensioner system with asynchronous gain-scheduled control is derived as

$$\begin{cases}\dot{z}(t)=\sum\limits_{i=1}^{3}\sum\limits_{j=1}^{3}\varsigma_i(t)\varsigma_j(t-\tau(t))(A_iz(t)+Dh(t))\\ \qquad+\sum\limits_{i=1}^{3}\sum\limits_{j=1}^{3}\varsigma_i(t)\varsigma_j(t-\tau(t))BK_j(1-\beta_k)d(t)\\ \qquad+\sum\limits_{i=1}^{3}\sum\limits_{j=1}^{3}\varsigma_i(t)\varsigma_j(t-\tau(t))BK_jz(t-\tau(t))\\ \qquad-\sum\limits_{i=1}^{3}\sum\limits_{j=1}^{3}\varsigma_i(t)\varsigma_j(t-\tau(t))BK_j\nu_k(t-\tau(t)),\\ \dot{d}(t)=0,\end{cases} \tag{10}$$

for $t\in\mathcal{F}_{k,i}$ $(i=0,1,\ldots,\mathcal{J}_k,\forall k\in\mathbb{N})$ with the reset equations

$$\begin{cases}z(f_{t_{k+1}})=z(f_{t_{k+1}}^-)=\lim\limits_{t\to f_{t_{k+1}}^-}z(t),\\ d(f_{t_{k+1}})=(1-\beta_k)d(f_{t_{k+1}}^-)+z(t_kh)-z(t_{k+1}h),\end{cases} \tag{11}$$

subject to

$$\begin{cases}t_{k+1}h-t_kh\le\varkappa,\\ \|\,\nu_k^{\mathrm{T}}(t-\tau(t))T^{\frac{1}{2}}\,\|\le\sigma\\ \quad\cdot\|\,(z^{\mathrm{T}}(t-\tau(t))-\nu_k^{\mathrm{T}}(t-\tau(t)))T^{\frac{1}{2}}\,\|\,.\end{cases} \tag{12}$$

The initial condition is supplemented as $z(t)=z(t_0h)$ $(t\in[t_0h-\eta_M,t_0h])$ and $d(t_0h)=-z(t_0h)$.

To suppress the adverse impact of friction force on the relative displacement z_i $(i=1,3,5)$ and ensure the safety of the riser system during the recoil response of the riser-tensioner system, the controlled output of system (10) is introduced as (Zhao et al., 2022a)

$$\eta(t)=C_0z(t)+D_0h(t), \tag{13}$$

where

$$C_0=\begin{bmatrix}1&0&0&0&0&0\\0&0&1&0&0&0\\0&0&0&0&1&0\end{bmatrix},\ D_0=\begin{bmatrix}-0.001\\-0.001\\-0.001\end{bmatrix}.$$

Therefore, the recoil control problem of the networked riser-tensioner system can be stated as follows:

AGSC (9) is designed such that (1) the system (Eqs. (10) and (11)) subject to condition (12) is exponentially mean-square stable when $h(t)=0$; i.e., the following inequalities hold for some $\upsilon_i>0$ $(i=1,2)$:

$$\mathbb{E}\{\|z(t)\|^2\}\le\upsilon_2\mathrm{e}^{-\upsilon_1(t-t_0h)}\mathbb{E}\{\|z(t_0h)\|^2+\|\eta(t_0h)\|^2\},$$

$$\mathbb{E}\{\|\eta(t)\|^2\}\le\upsilon_2\mathrm{e}^{-\upsilon_1(t-t_0h)}\mathbb{E}\{\|z(t_0h)\|^2+\|\eta(t_0h)\|^2\}.$$

(2) Under the zero initial condition, $\mathbb{E}\{\|\eta(t)\|_2\}\le\gamma\|h(t)\|_2$ holds for the nonzero $h(t)$ and the prescribed H_∞ performance level $\gamma>0$.

3 Main results

In this section, Lemma 2 shows a computing method of the asynchronous deviation bounds, and Theorems 1 and 2 provide the disturbance attenuation analysis and asynchronous gain-scheduled control design, respectively.

3.1 Computing method of asynchronous deviation bounds of scheduling parameters

Lemma 2 For given $\eta_M > 0$ and $\varsigma_i(t)$ $(i = 1, 2, 3)$ given in Lemma 1, the following inequality holds:

$$|\varsigma_i(t) - \varsigma_i(t - \tau(t))| \le \mu_i,\ i = 1, 2, 3, \tag{14}$$

where the asynchronous deviation bound $\mu_i = \min\{1, \eta_M v_i\}$ $(i = 1, 2, 3)$ and

$$v_1 = \max_{t\in[0,\infty)} \left| \frac{\dot{z}_1(t)}{\left(\frac{1}{\underline{q}_2} - \frac{1}{\overline{q}_2}\right)\left(z_1(t) + \frac{A_{\mathrm{p}}\bar{z}_{01} - V_{\mathrm{L}_0}}{A_{\mathrm{p}}}\right)^2} \right|,$$

$$v_2 = \max_{t\in[0,\infty)} \left| \frac{\dot{z}_1(t)}{\left(\frac{1}{\underline{q}_2} - \frac{1}{\overline{q}_2}\right)\left(z_1(t) + \frac{A_{\mathrm{p}}\bar{z}_{01} - V_{\mathrm{L}_0}}{A_{\mathrm{p}}}\right)^2} \right| + \max_{t\in[0,\infty)} \left| \frac{\dot{z}_1(t)}{\left(\frac{1}{\underline{q}_1} - \frac{1}{\overline{q}_1}\right)\left(z_1(t) + \frac{V_{\mathrm{H}_0} + A_{\mathrm{r}}\bar{z}_{01}}{A_{\mathrm{r}}}\right)^2} \right|,$$

$$v_3 = \max_{t\in[0,\infty)} \left| \frac{\dot{z}_1(t)}{\left(\frac{1}{\underline{q}_1} - \frac{1}{\overline{q}_1}\right)\left(z_1(t) + \frac{V_{\mathrm{H}_0} + A_{\mathrm{r}}\bar{z}_{01}}{A_{\mathrm{r}}}\right)^2} \right|.$$

Proof It is clear that

$$|\varsigma_i(t) - \varsigma_i(t - \tau(t))| \le \max_{t\in[0,\infty)} \left\{ \left| \frac{\partial \varsigma_i}{\partial z_1(t)} \dot{z}_1(t) \right| \right\} \tau(t). \tag{15}$$

Based on the functional relations between $\varsigma_i(t)$ and $z_1(t)$ given in Lemma 1, one has $|\varsigma_i(t) - \varsigma_i(t - \tau(t))| \le \eta_M v_i$ $(i = 1, 2, 3)$ from condition (15). Considering $0 \le \varsigma_i(t) \le 1$ $(i = 1, 2, 3)$, one can complete the proof.

3.2 Disturbance attenuation analysis of the networked riser-tensioner system

Theorem 1 For given positive scalars h, τ_M, η_M, γ, $\varkappa$, $\sigma \in (0, 1)$, $\beta \in (0, 1]$, $\mu_i \in [0, 1]$ $(i = 1, 2, 3)$, and matrix K_i $(i = 1, 2, 3)$, the system (Eqs. (10) and (11)) subject to condition (12) is exponentially mean-square stable with H_∞ performance γ, if there exist symmetric matrices $P > 0$, $Q > 0$, $R > 0$, $S > 0$, $T > 0$, $H < 0$, $W > 0$, $G_i > 0$ $(i = 1, 2, 3)$, $M_i > 0$ $(i = 1, 2, 3)$, $N_i > 0$ $(i = 1, 2, 3)$, and matrices U_i $(i = 1, 2, 3)$ and X_i $(i = 1, 2)$ such that the following linear matrix inequalities (LMIs) hold for $l = 1, 2, 3, 4$ and $i, j = 1, 2, 3$:

$$\Pi_i > 0, \tag{16}$$

$$\Xi_{lij} < 0, \tag{17}$$

$$2N_i - H^{(i,j)} - H^{(j,i)} > 0, \tag{18}$$

$$2M_j + H^{(i+3,j+3)} + H^{(j+3,i+3)} > 0, \tag{19}$$

where $\Pi_i \in \mathbb{R}^{2n\times 2n}$ $(i = 1, 2)$, $\Pi_3 \in \mathbb{R}^{3n\times 3n}$ $(n = 6)$, $\Xi_{lij} \in \mathbb{R}^{(12n+1)\times(12n+1)}$ $(l = 1, 3)$, $\Xi_{lij} \in \mathbb{R}^{(14n+1)\times(14n+1)}$ $(l = 2, 4)$, $H^{(i,j)} \in \mathbb{R}^{3n\times 3n}$ $(i, j = 1, 2, \ldots, 6)$ are block matrices, $\mathbb{R}$ denotes the set of real numbers, and $(\star)^{(s,t)}$ represents the block matrix of the s^{th} row and t^{th} column of matrix $(\star)$. In addition,

$$\Pi_1^{(1,1)} = G_3 + hG_2,$$
$$\Pi_2^{(1,1)} = G_3 + (h + \tau_M)G_2,$$
$$\Pi_3^{(1,1)} = \begin{bmatrix} (2\beta - \beta^2)G_1 - \omega W & -(1 - \beta)G_1 \\ \star & G_3 - G_1 \end{bmatrix},$$
$$\Pi_1^{(1,2)} = \Pi_2^{(1,2)} = -G_3,$$
$$\Pi_3^{(1,2)} = \mathrm{col}\{0, -G_3\},$$
$$\Pi_1^{(2,2)} = G_3,$$
$$\Pi_2^{(2,2)} = G_3 - \tau_M G_2,$$
$$\Pi_3^{(2,2)} = G_3 + hG_2,$$
$$\Xi_{1ij}^{(1,1)} = \Psi_{ij},$$
$$\Xi_{2ij}^{(1,1)} = \Psi_{ij} + \tau_M(\Psi_1 + \Psi_2),$$
$$\Xi_{3ij}^{(1,1)} = \Psi_{ij} + \eta_M\Psi_1,$$
$$\Xi_{4ij}^{(1,1)} = \Psi_{ij} + \eta_M\Psi_1 + \tau_M\Psi_2,$$
$$\Xi_{1ij}^{(1,2)} = \eta_M U_3,$$
$$\Xi_{2ij}^{(1,2)} = [\tau_M U_2 \quad hU_3],$$
$$\Xi_{3ij}^{(1,2)} = \eta_M U_1,$$
$$\Xi_{4ij}^{(1,2)} = [hU_1 \quad \tau_M U_2],$$
$$\Xi_{lij}^{(1,3)} = (\epsilon_1^{\mathrm{T}} X_1 + \epsilon_2^{\mathrm{T}} X_2)D + \epsilon_1^{\mathrm{T}} C_0^{\mathrm{T}} D_0,$$
$$\Xi_{1ij}^{(2,2)} = \mathrm{diag}\{-\eta_M R, -3\eta_M R\},$$
$$\Xi_{2ij}^{(2,2)} = \mathrm{diag}\{-\tau_M R, -3\tau_M R, -hR, -3hR\},$$
$$\Xi_{3ij}^{(2,2)} = \mathrm{diag}\{-\eta_M R_s, -3\eta_M R_s\},$$
$$\Xi_{4ij}^{(2,2)} = \mathrm{diag}\{-hR_s, -3hR_s, -\tau_M R, -3\tau_M R\},$$
$$\Xi_{1ij}^{(2,3)} = \Xi_{3ij}^{(2,3)} = 0_{2n\times 1},$$
$$\Xi_{2ij}^{(2,3)} = \Xi_{4ij}^{(2,3)} = 0_{4n\times 1},$$
$$\Xi_{lij}^{(3,3)} = -\gamma^2 + D_0^{\mathrm{T}} D_0,$$

$$
\begin{aligned}
&\tau_M=\eta_M-h,\quad \omega=\varkappa+\tau_M,\\
&\Psi_{ij}=\Psi_0-\epsilon_4^{\mathrm{T}}T\epsilon_4+\sigma^2(\epsilon_3-\epsilon_4)^{\mathrm{T}}T(\epsilon_3-\epsilon_4)\\
&\qquad-\varphi_{11}^{\mathrm{T}}\Omega_{ij}\varphi_{11}+\epsilon_1^{\mathrm{T}}C_0^{\mathrm{T}}C_0\epsilon_1\\
&\qquad-\mathrm{Sym}\{(\epsilon_1^{\mathrm{T}}X_1+\epsilon_2^{\mathrm{T}}X_2)\epsilon_2\}\\
&\qquad+\mathrm{Sym}\{U_1\Gamma\varphi_7+U_2\Gamma\varphi_8+U_3\Gamma\varphi_{10}\}\\
&\qquad+\mathrm{Sym}\{(\epsilon_1^{\mathrm{T}}X_1+\epsilon_2^{\mathrm{T}}X_2)(A_i\epsilon_1+BK_j\mathcal{E})\},\\
&\mathcal{E}=\epsilon_3-\epsilon_4+(1-\beta)\epsilon_{10},\\
&\Psi_0=\epsilon_1^{\mathrm{T}}Q\epsilon_1+h\epsilon_2^{\mathrm{T}}G_3\epsilon_2+\epsilon_4^{\mathrm{T}}G_2\epsilon_4-\epsilon_5^{\mathrm{T}}Q\epsilon_5\\
&\qquad+\eta_M\epsilon_2^{\mathrm{T}}R\epsilon_2+\eta_M\varphi_9^{\mathrm{T}}S\varphi_9-\epsilon_{10}^{\mathrm{T}}W\epsilon_{10}\\
&\qquad+\mathrm{Sym}\{\varphi_1^{\mathrm{T}}P\varphi_2-\varphi_5^{\mathrm{T}}S\varphi_6\},\\
&\Psi_1=-\varphi_9^{\mathrm{T}}S\varphi_9-\varphi_6^{\mathrm{T}}S\varphi_6+\mathrm{Sym}\{\varphi_1^{\mathrm{T}}P\varphi_3\},\\
&\Psi_2=\varphi_6^{\mathrm{T}}S\varphi_6+\mathrm{Sym}\{\varphi_1^{\mathrm{T}}P\varphi_4\},\\
&\Omega_{ij}=H^{(i,j+3)}+\frac{H^{(i,j)}+H^{(j,i)}}{2}\\
&\qquad+H^{(j+3,i)}+\frac{H^{(i+3,j+3)}+H^{(j+3,i+3)}}{2}\\
&\qquad-\sum_{l=1}^{3}\mu_l\left(N_i-\frac{H^{(i,l)}+H^{(l,i)}}{2}+M_j\right)\\
&\qquad-\sum_{l=1}^{3}\mu_l\left(\frac{H^{(j+3,l+3)}+H^{(l+3,j+3)}}{2}\right),\\
&R_s=R+S_{11},\\
&S_{11}=\left[\begin{array}{ccc}I&0&0\end{array}\right]S\left[\begin{array}{ccc}I&0&0\end{array}\right]^{\mathrm{T}},\\
&\Gamma=\left[\begin{array}{ccc}I&-I&0\\I&I&-2I\end{array}\right],\\
&\varphi_1=\mathrm{col}\{\epsilon_2,\epsilon_1-\epsilon_5\},\quad \varphi_2=\mathrm{col}\{\epsilon_1,\eta_M\epsilon_9\},\\
&\varphi_3=\mathrm{col}\{0,\epsilon_7-\epsilon_9\},\quad \varphi_4=\mathrm{col}\{0,\epsilon_8-\epsilon_7\},\\
&\varphi_5=\mathrm{col}\{\epsilon_1-\epsilon_6,0,0\},\quad \varphi_6=\mathrm{col}\{0,\epsilon_3,\epsilon_6\},\\
&\varphi_7=\mathrm{col}\{\epsilon_1,\epsilon_6,\epsilon_7\},\quad \varphi_8=\mathrm{col}\{\epsilon_6,\epsilon_3,\epsilon_8\},\\
&\varphi_9=\mathrm{col}\{\epsilon_2,\epsilon_3,\epsilon_6\},\quad \varphi_{10}=\mathrm{col}\{\epsilon_3,\epsilon_5,\epsilon_9\},\\
&\varphi_{11}=\mathrm{col}\{\epsilon_1,\epsilon_2,\epsilon_3\},\\
&\epsilon_i=\left[\begin{array}{ccc}0_{n\times(i-1)n}&I_n&0_{n\times(10-i)n}\end{array}\right].
\end{aligned}
$$

Here, $\mathrm{Sym}\{\star\}=\star+\star^{\mathrm{T}}$. The proof of Theorem 1 is given in the supplementary materials.

3.3 Nonlinear design of the networked AGSC

Theorem 2 For a given scalar ϱ, and positive scalars h, τ_M, η_M, γ, $\varkappa$, $\sigma\in(0,1)$, $\beta\in(0,1]$, $\mu_i\in[0,1]$ $(i=1,2,3)$, there exists controller (6), which can ensure that the system (Eqs. (10) and (11)) subject to condition (12) is exponentially mean-square stable with H_∞ performance level γ, if there exist symmetric matrices $\tilde{P}>0$, $\tilde{Q}>0$, $\tilde{R}>0$, $\tilde{S}>0$, $\tilde{T}>0$, $\tilde{H}<0$, $\tilde{W}>0$, $\tilde{G}_i>0$ $(i=1,2,3)$, $\tilde{M}_i>0$ $(i=1,2,3)$, $\tilde{N}_i>0$ $(i=1,2,3)$, and matrices $\tilde{U}_i$ $(i=1,2,3)$, X, and Y_i $(i=1,2,3)$, such that the following LMIs hold for $l=1,2,3,4$ and $i,j=1,2,3$:

$$\tilde{\Pi}_i>0, \tag{20}$$

$$\tilde{\Xi}_{lij}<0, \tag{21}$$

$$2\tilde{N}_i-\tilde{H}^{(i,j)}-\tilde{H}^{(j,i)}>0, \tag{22}$$

$$2\tilde{M}_j+\tilde{H}^{(i+3,j+3)}+\tilde{H}^{(j+3,i+3)}>0, \tag{23}$$

where

$$
\begin{aligned}
&\tilde{\Xi}_{1ij}^{(1,1)}=\tilde{\Psi}_{ij},\\
&\tilde{\Xi}_{2ij}^{(1,1)}=\tilde{\Psi}_{ij}+\tau_M(\tilde{\Psi}_1+\tilde{\Psi}_2),\\
&\tilde{\Xi}_{3ij}^{(1,1)}=\tilde{\Psi}_{ij}+\eta_M\tilde{\Psi}_1,\\
&\tilde{\Xi}_{4ij}^{(1,1)}=\tilde{\Psi}_{ij}+\eta_M\tilde{\Psi}_1+\tau_M\tilde{\Psi}_2,\\
&\tilde{\Psi}_{ij}=\tilde{\Psi}_0-\epsilon_4^{\mathrm{T}}\tilde{T}\epsilon_4+\sigma^2(\epsilon_3-\epsilon_4)^{\mathrm{T}}\tilde{T}(\epsilon_3-\epsilon_4)\\
&\qquad-\varphi_{11}^{\mathrm{T}}\tilde{\Omega}_{ij}\varphi_{11}+\mathrm{Sym}\{\tilde{U}_1\Gamma\varphi_7+\tilde{U}_2\Gamma\varphi_8\}\\
&\qquad+\mathrm{Sym}\{\tilde{U}_3\Gamma\varphi_{10}+(\epsilon_1^{\mathrm{T}}+\varrho\epsilon_2^{\mathrm{T}})A_iX\varepsilon_1\}\\
&\qquad+\mathrm{Sym}\{(\epsilon_1^{\mathrm{T}}+\varrho\epsilon_2^{\mathrm{T}})(BY_j\mathcal{E}-X\epsilon_2)\},
\end{aligned}
$$

and $\tilde{\Xi}_{lij}^{(1,2)}$, $\tilde{\Xi}_{lij}^{(1,3)}$, $\tilde{\Xi}_{lij}^{(2,2)}$, $\tilde{\Xi}_{lij}^{(2,3)}$, $\tilde{\Xi}_{lij}^{(3,3)}$, $\tilde{\Psi}_0$, $\tilde{\Psi}_1$, $\tilde{\Psi}_2$, $\tilde{\Omega}_{ij}$, $\tilde{\Pi}_i$ are given by replacing the matrix variables $(\star)$ in $\Xi_{lij}^{(1,2)}$, $\Xi_{lij}^{(1,3)}$, $\Xi_{lij}^{(2,2)}$, $\Xi_{lij}^{(2,3)}$, $\Xi_{lij}^{(3,3)}$, Ψ_0, Ψ_1, Ψ_2, Ω_{ij}, Π_i by $(\tilde{\star})$, respectively; moreover, the gain matrix of controller (6) is calculated as $K_i=Y_iX^{-1}$ $(i=1,2,3)$ and the weighting matrix of the event-triggered scheme (7) is calculated as $T=X^{-\mathrm{T}}\tilde{T}X^{-1}$.

The proof of Theorem 2 is given in the supplementary materials.

Remark 1 The differences between the proposed results and the existing ones in Zhao et al. (2022a, 2022b) and Zhang W et al. (2023a, 2023b) are reflected in two aspects: (1) The system models and corresponding recoil control methods of the riser-tensioner system are different. In Zhao et al. (2022a, 2022b) and Zhang W et al. (2023a, 2023b), a linearization method based on the Taylor expansion was used to deal with the nonlinear tension force of the tensioner and linear control strategies were proposed for the linearized riser-tensioner system, while a nonlinear LPV system is presented in this study to equivalently describe the nonlinear tension force and a nonlinear controller is tailored to handle the modeling nonlinearity. (2) The system framework and control constraints are different. In Zhao

et al. (2022a, 2022b) and Zhang W et al. (2023a, 2023b), a traditional system control architecture of the riser-tensioner system was discussed, while the NCS paradigm is considered in this study and the effect of event-triggered communication, data loss, and communication delay on control performance is investigated. In particular, the traditional recoil control method of the riser-tensioner system does not work in the NCS framework, as will be illustrated in the numerical example.

Remark 2 The analysis and design results, i.e., Theorems 1 and 2, are applicable to general LPV systems if Lemma 2 can be applied. In this case, it is necessary to update the system matrices in $\Xi_{lij}^{(1,1)}$, $\Xi_{lij}^{(1,3)}$, $\Xi_{lij}^{(3,3)}$, $\tilde{\Xi}_{lij}^{(1,1)}$, $\tilde{\Xi}_{lij}^{(1,3)}$, $\tilde{\Xi}_{lij}^{(3,3)}$, revise the size of n, and adjust the corresponding dimensions of matrix variables. Since the scheduling parameters in general LPV systems are usually functions of system states and the upper bound η_M is prior knowledge, condition (14) in Lemma 2 can be satisfied.

4 Simulation results

In this section, we provide numerical results to demonstrate that the proposed nonlinear recoil control method is characterized by less conservatism and a better control effect in comparison with the existing linear control method.

First, the parameter values of the riser-tensioner system (Eqs. (1) and (2)) are listed in Table 1. Using these parameter values, the system matrices in Eq. (5) can be easily calculated. It is assumed that the displacement and velocity of the riser-tensioner system satisfy $-6\ \text{m} \le z_i(t) \le 2.5\ \text{m}$ $(i=1,3,5)$, $-2\ \text{m/s} \le z_i(t) \le 2.5\ \text{m/s}$ $(i=2,4,6)$. Using Lemma 2, one can obtain the asynchronous deviation bound μ_i $(i=1,2,3)$ for a given η_M.

Table 1 Numerical values of physical parameters in the riser-tensioner system (Zhao et al., 2022a, 2022b)

Parameter	Value	Parameter	Value
P_{H_0}	3.05 MPa	f_{m}	0.004
V_{H_0}	4.28 m^3	L_{r}	1000 m
P_{L_0}	0.15 MPa	g	9.8 N/kg
V_{L_0}	2.25 m^3	D_{e}	0.4826 m
A_{r}	0.2048 m^2	F_{b_1}	2 929 435.6 N
A_{p}	0.2463 m^2	F_{b_2}	2 908 777.2 N
m_1	355 206 kg	F_{b_3}	3 001 838.0 N
m_2	327 124 kg	k_2	16 686 000 N/m
m_3	456 620 kg	k_3	16 686 000 N/m
A_{s}	0.0405 m^2	c_1	134 435.3395 N·s/m
ρ_{w}	1025 kg/m^3	c_2	46 726.3997 N·s/m
ρ_{m}	1537 kg/m^3	c_3	55 205.6567 N·s/m
f_{w}	0.002		

Second, we evaluate the solvability of the proposed nonlinear control design and the linear control design in Zhao et al. (2022a). Using the design method in Zhao et al. (2022a), a linear PDHC is proposed for a riser-tensioner system, where PDHC means that a pure time-varying delay $\tau(t)$ satisfying $0 \le \tau(t) \le \eta_M$ is artificially introduced into the control input $u(t) = Kz(t-\tau(t))$ under a traditional system framework. Concerning the present research, Theorem 2 can provide a nonlinear AGSC for the networked riser-tensioner system. For given $\gamma = 1.0$, the maximum allowable delay bound (MADB) can be obtained as $\eta_M = 0.095$ s by using the method in Zhao et al. (2022a). For given $\gamma = 1.0$, $h = 0.01$ s, $\varkappa = 0.2$ s, $\beta = 0.9$, $\sigma = 0.1$, and $\varrho = 0.2$, the MADB can be obtained as $\eta_M = 0.395$ s by using Theorem 2. From the design feasibility, one can ascertain that the proposed nonlinear control design method is less conservative than the linear control design method in Zhao et al. (2022a).

Third, we demonstrate that the proposed nonlinear AGSC can achieve a better recoil control effect of the networked riser-tensioner system than the linear PDHC in Zhao et al. (2022a). In the following, we will compare the control effect of nonlinear AGSC and linear PDHC in two cases of η_M.

Case 1: $\eta_M = 0.095$ s. This involves using the method in Zhao et al. (2022a) to obtain the minimum $\gamma_{\min} = 0.002$ and the following control gain:

$$K = 10^5 \times \begin{bmatrix} -0.0311 & 3.2719 & 0.5663 \\ -3.9999 & -0.0832 & 3.2402 \end{bmatrix}. \tag{24}$$

Such a controller is denoted by PDHC-0095.

Under $h = 0.01$ s, $\varkappa = 0.2$ s, $\beta = 0.9$, $\sigma = 0.1$, and $\varrho = 0.2$, Theorem 2 can be used to obtain the minimum $\gamma_{\min} = 0.001\,75$ and the following control gains:

$$\begin{cases} K_1 = 10^6 \times \begin{bmatrix} 1.6513 & 1.6166 & 3.7702 \\ 1.1566 & 3.2397 & 1.5592 \end{bmatrix}, \\ K_2 = 10^6 \times \begin{bmatrix} 1.5169 & 1.5338 & 3.5481 \\ 1.1017 & 3.1260 & 1.4866 \end{bmatrix}, \\ K_3 = 10^6 \times \begin{bmatrix} 1.4765 & 1.5853 & 3.6599 \\ 1.1463 & 3.1038 & 1.5474 \end{bmatrix}. \end{cases} \tag{25}$$

Such a controller is denoted by AGSC-0095.

Case 2: $\eta_M = 0.395$ s. Under $\gamma = 1.0$, $h = 0.01$ s, $\varkappa = 0.2$ s, $\beta = 0.9$, $\sigma = 0.1$, and $\varrho = 0.2$, Theorem 2 can be used to obtain the following control gains:

$$\begin{cases} K_1 = 10^5 \times [\ 1.0518 \quad 2.4574 \quad 0.1529 \\ \qquad\qquad 2.3226 \quad 0.2748 \quad 3.2926\ ], \\ K_2 = 10^5 \times [\ 1.0517 \quad 2.4574 \quad 0.1528 \\ \qquad\qquad 2.3226 \quad 0.2747 \quad 3.2926\ ], \\ K_3 = 10^5 \times [\ 1.0518 \quad 2.4574 \quad 0.1529 \\ \qquad\qquad 2.3227 \quad 0.2748 \quad 3.2927\ ]. \end{cases} \tag{26}$$

Such a controller is denoted by AGSC-0395. In this case, the design method in Zhao et al. (2022a) is not feasible.

In simulations, for given $\Delta t = 0.01$ s, $a(0) = 0$ m/s^2, $v(0) = 0$ m/s, and $L_{\mathrm{w}}(0) = 0$ m, the external force $h(t)$ in system (4) is approximately solved by using the whole fluid model of drilling mud discharge in Li CW et al. (2016) and Zhao et al. (2022a, 2022b). The recoil responses of the riser-tensioner system with the designed controllers in cases 1 and 2 are depicted in Figs. 1 and 2, respectively. As demonstrated in Fig. 1, for $\eta_M = 0.095$ s, the achieved stabilizing transient time is approximately 10, 60, and 80 s, corresponding to the AGSC-0095 designed in the present study, the PDHC-0095 introduced in Zhao et al. (2022a), and absence of controller, respectively. It indicates that AGSC-0095 ensures a better recoil response of the riser-tensioner system compared with PDHC-0095 and absence of control. Meanwhile, the simulation value γ_{sim} and the theoretical value $\gamma_{\min}$ of the H_∞ performance index provided by AGSC-0095 and PDHC-0095 are compared in Table 2, which verifies that AGSC-0095 can ensure a better interference rejection capability. When $\eta_M = 0.395$ s, the stabilizing transient time of the AGSC-0395 is about 60 s, while the design method in Zhao et al. (2022a) does not work. Based on the simulations conducted for the two cases, one can conclude that the proposed networked LPV controller can satisfactorily complete the control task and effectively suppress the recoil response of the riser-tensioner system, compared with the existing linear recoil controller. For given $\beta = 0.9$ and $\varkappa = 0.2$ s, Figs. 3 and 4 depict the release time and release interval of the hybrid event-triggered scheme (12) in

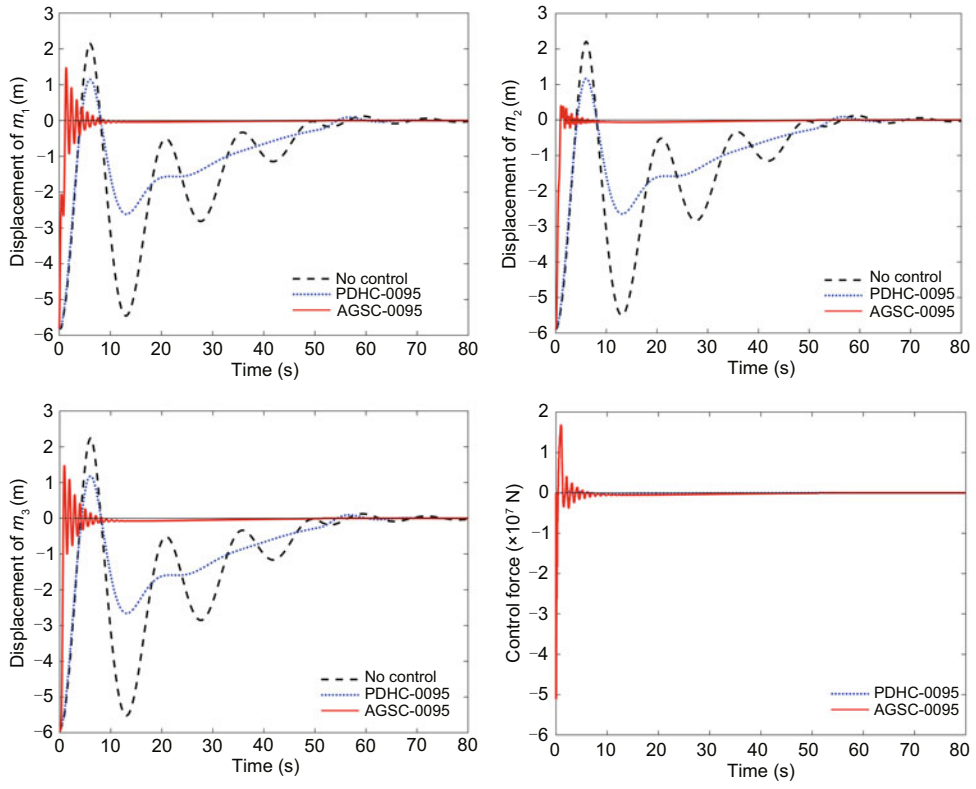

Fig. 1 Displacements and control force of the riser system without control, with AGSC-0095, and with PDHC-0095

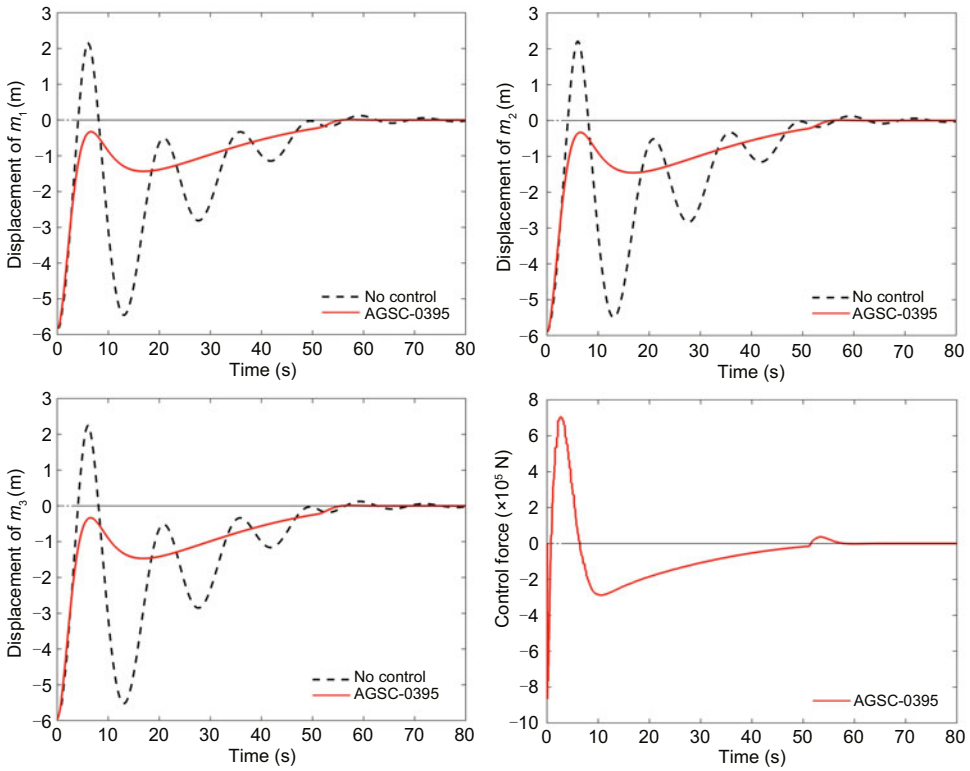

Fig. 2 Displacements and control force of the riser system without control and with AGSC-0395

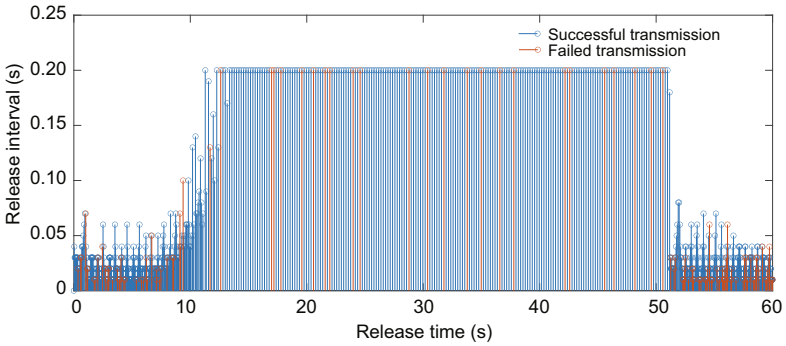

Fig. 3 Release time and release interval when $\varkappa = 0.2$ s, $\beta = 0.9$, and $\eta_M = 0.095$ s (References to color refer to the online version of this figure)

cases 1 and 2, respectively. It can be seen that the sampled data $z(t_k h + \varkappa)$ $(\forall k \in \mathbb{N})$ are compulsorily triggered when $\varkappa = 0.2$ s is reached. The advantage that the proposed event-triggered control can tolerate the random data loss of triggered data is verified. When $\eta_M = 0.095$ s (or 0.395 s), the average data transmission interval of AGSC-0095 (or AGSC-0395) can be calculated as 0.0506 s (or 0.0606 s) and the amount of data transferred of AGSC-0095 (or AGSC-0395) is reduced by 80.2500% (or 87.6250%) in comparison with the results obtained for the time-triggered control with $h = 0.01$ s. The advantage that the proposed event-triggered control can significantly save communication and computing resources is also confirmed.

Table 2 H_∞ performance indexes of the asynchronous gain-scheduled controller (AGSC) and pure delayed H_∞ controller (PDHC) with $\tau_M = 0.095$ s

Controller	$\gamma_{\min}$	γ_{sim}
PDHC	0.002	0.001 75
AGSC	0.001 748	0.001 733

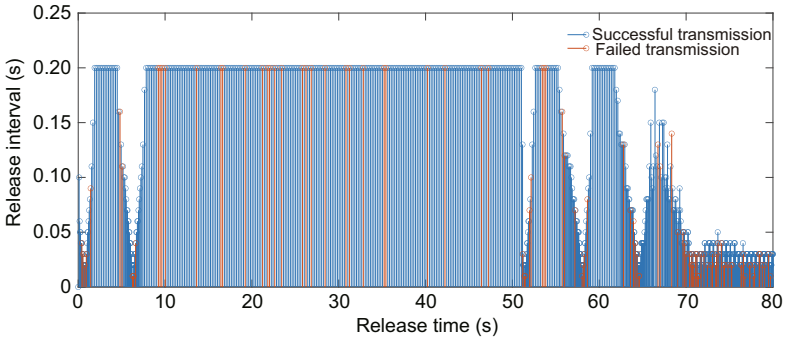

Fig. 4 Release time and release interval when $\varkappa = 0.2$ s, $\beta = 0.9$, and $\eta_M = 0.395$ s (References to color refer to the online version of this figure)

5 Conclusions

This paper has proposed nonlinear networked system modeling and asynchronous gain-scheduled control methods of the riser-tensioner system with event-triggered sampling, communication delay, and random data loss. The nonlinearities from the tension force have been modeled by a triangle-based polytope LPV system. The networked constraints have been reflected by an asynchronous parameter-scheduled system with sampling and random impulsive updates. To suppress the recoil response of the riser-tensioner system subject to friction force and network constraints, an asynchronous gain-scheduled control design algorithm that depends on deviation bounds has been proposed in the H_∞ control sense. Numerical results have been provided to verify that the nonlinear networked system modeling and control methods are better than the linear control method.

Contributors

Dawei ZHANG and Shuqian ZHU designed the research. Na PANG processed the data and drafted the paper. Dawei ZHANG and Shuqian ZHU revised and finalized the paper.

Compliance with ethics guidelines

Na PANG, Dawei ZHANG, and Shuqian ZHU declare that they have no conflict of interest.

Data availability

The data that support the findings of this study are available from the corresponding author on reasonable request.

References

Chu SQ, Xie ZC, Wong PK, et al., 2022. Observer-based gain scheduling path following control for autonomous electric vehicles subject to time delay. *Veh Syst Dyn*, 60(5):1602-1626. https://doi.org/10.1080/00423114.2020.1864419

Coutinho PHS, Palhares RM, 2021. Dynamic periodic event-triggered gain-scheduling control co-design for quasi-LPV systems. *Nonl Anal Hybrid Syst*, 41:101044. https://doi.org/10.1016/j.nahs.2021.101044

Dinh TQ, Ahn KK, Marco J, 2017. A novel robust predictive control system over imperfect networks. *IEEE Trans Ind Electron*, 64(2):1751-1761. https://doi.org/10.1109/TIE.2016.2580124

Gao ZF, Wu T, Zhang DW, et al., 2022. Network-based gain-scheduled control for preview path tracking of autonomous electric vehicles subject to communication delays. *Int J Syst Sci*, 53(12):2549-2565. https://doi.org/10.1080/00207721.2021.2005177

Gao ZF, Zhang DW, Zhu SQ, 2023. Hybrid event-triggered synchronization control of delayed chaotic neural networks against communication delay and random data loss. *Chaos Sol Fract*, 172:113535. https://doi.org/10.1016/j.chaos.2023.113535

Ge XH, Han QL, Wang ZD, 2019. A dynamic event-triggered transmission scheme for distributed set-membership estimation over wireless sensor networks. *IEEE Trans Cybern*, 49(1):171-183. https://doi.org/10.1109/TCYB.2017.2769722

Ge XH, Han QL, Zhang XM, et al., 2020. Distributed event-triggered estimation over sensor networks: a survey. *IEEE Trans Cybern*, 50(3):1306-1320. https://doi.org/10.1109/TCYB.2019.2917179

Ge XH, Han QL, Zhang XM, et al., 2021. Dynamic event-triggered control and estimation: a survey. *Int J Autom Comput*, 18(6):857-886. https://doi.org/10.1007/s11633-021-1306-z

Ge XH, Xiao SY, Han QL, et al., 2022. Dynamic event-triggered scheduling and platooning control co-design for automated vehicles over vehicular ad-hoc networks. *IEEE/CAA J Autom Sin*, 9(1):31-46. https://doi.org/10.1109/JAS.2021.1004060

He WL, Mo ZK, Han QL, et al., 2020. Secure impulsive synchronization in Lipschitz-type multi-agent systems subject to deception attacks. *IEEE/CAA J Autom Sin*, 7(5):1326-1334. https://doi.org/10.1109/JAS.2020.1003297

Hu SL, Yue D, Han QL, et al., 2020. Observer-based event-triggered control for networked linear systems subject to denial-of-service attacks. *IEEE Trans Cybern*, 50(5):1952-1964. https://doi.org/10.1109/TCYB.2019.2903817

Jiang YH, Wu W, Lou XY, et al., 2021. Event-based H_∞ control for piecewise-affine systems subject to actuator saturation. *Front Inform Technol Electron Eng*, 22(5):720-731. https://doi.org/10.1631/FITEE.1900601

Li CW, Fan HH, Wang ZM, et al., 2016. Two methods for simulating mud discharge after emergency disconnection of a drilling riser. *J Nat Gas Sci Eng*, 28:142-152. https://doi.org/10.1016/j.jngse.2015.11.038

Li WF, Xie ZC, Zhao J, et al., 2020. Velocity-based robust fault tolerant automatic steering control of autonomous ground vehicles via adaptive event triggered network communication. *Mech Syst Signal Process*, 143:106798. https://doi.org/10.1016/j.ymssp.2020.106798

Liu J, Zhao HL, Liu QY, et al., 2018. Dynamic behavior of a deepwater hard suspension riser under emergency evacuation conditions. *Ocean Eng*, 150:138-151. https://doi.org/10.1016/j.oceaneng.2017.12.050

Liu XQ, Li YW, Zhang N, et al., 2020. Improved axial dynamic analysis of risers based on finite element method and data-driven models. *Ocean Eng*, 214:107782. https://doi.org/10.1016/j.oceaneng.2020.107782

Liu XQ, Liu ZW, Wang XL, et al., 2021. Recoil control of deepwater drilling riser system based on optimal control theory. *Ocean Eng*, 220:108473. https://doi.org/10.1016/j.oceaneng.2020.108473

Liu XQ, Liu ZW, Wang XL, et al., 2022. An intelligent recoil controller for riser system based on fuzzy control theory. *Int J Naval Archit Ocean Eng*, 14:100439. https://doi.org/10.1016/j.ijnaoe.2022.100439

Liu Y, Wang YN, Feng YH, et al., 2022. Neural network-based adaptive boundary control of a flexible riser with input deadzone and output constraint. *IEEE Trans Cybern*, 52(12):13120-13128. https://doi.org/10.1109/TCYB.2021.3102160

Liu ZQ, Lou XY, Jia JJ, 2022. Event-triggered dynamic output-feedback control for a class of Lipschitz nonlinear systems. *Front Inform Technol Electron Eng*, 23(11):1684-1699. https://doi.org/10.1631/FITEE.2100552

Ma H, Tang GY, Ding XQ, 2019. Modified-transformation-based networked controller for offshore platforms under multiple outloads. *Ocean Eng*, 190:106392. https://doi.org/10.1016/j.oceaneng.2019.106392

Meng S, Chen Y, Che CD, 2020. Coupling effects of a deepwater drilling riser and the platform and the discharging fluid column in an emergency disconnect scenario. *China Ocean Eng*, 34(1):21-29. https://doi.org/10.1007/s13344-020-0003-y

Pestana RG, Roveri FE, Franciss R, et al., 2016. Marine riser emergency disconnection analysis using scalar elements for tensioner modelling. *Appl Ocean Res*, 59:83-92. https://doi.org/10.1016/j.apor.2016.05.004

Shi YC, Tian EG, Shen SB, et al., 2021. Adaptive memory-event-triggered H_∞ control for network-based T-S fuzzy systems with asynchronous premise constraints. *IET Contr Theory Appl*, 15(4):534-544. https://doi.org/10.1049/cth2.12059

Sun YN, Zou WC, Guo J, et al., 2021. Containment control for heterogeneous nonlinear multi-agent systems under distributed event-triggered schemes. *Front Inform Technol Electron Eng*, 22(1):107-119. https://doi.org/10.1631/FITEE.2000034

Wang T, Liu YJ, 2018. Dynamic response of platform-riser coupling system with hydro-pneumatic tensioner. *Ocean Eng*, 166:172-181. https://doi.org/10.1016/j.oceaneng.2018.08.004

Wang XL, Liu XQ, Zhang N, et al., 2021. Improved recoil dynamic analysis of the deepwater riser system after emergency disconnection. *Appl Ocean Res*, 113:102719. https://doi.org/10.1016/j.apor.2021.102719

Wang XL, Liu XQ, Liu ZW, et al., 2022. Dynamic recoil response of tensioner and riser coupled in an emergency disconnection scenario. *Ocean Eng*, 247:110730. https://doi.org/10.1016/j.oceaneng.2022.110730

Wang YB, Gao DL, 2019. Recoil analysis of deepwater drilling riser after emergency disconnection. *Ocean Eng*, 189:106406. https://doi.org/10.1016/j.oceaneng.2019.106406

Wei Y, Luo J, Yan HC, et al., 2021. Event-triggered adaptive finite-time control for nonlinear systems under asymmetric time-varying state constraints. *Front Inform Technol Electron Eng*, 22(12):1610-1624. https://doi.org/10.1631/FITEE.2000692

Zhang BL, Cao EZ, Cai ZH, et al., 2021. Event-triggered H_∞ control for networked spar-type floating production platforms with active tuned heave plate mechanisms and deception attacks. *J Franklin Inst*, 358(7):3554-3584. https://doi.org/10.1016/j.jfranklin.2021.02.035

Zhang DW, Han QL, Zhang XM, 2020. Network-based modeling and proportional-integral control for direct-drive-wheel systems in wireless network environments. *IEEE Trans Cybern*, 50(6):2462-2474. https://doi.org/10.1109/TCYB.2019.2924450

Zhang W, Zhang BL, Han QL, et al., 2023a. Observer-based dynamic optimal recoil controller design for deepwater drilling riser systems. *Ocean Eng*, 267:113324. https://doi.org/10.1016/j.oceaneng.2022.113324

Zhang W, Zhang BL, Han QL, et al., 2023b. Recoil attenuation for deepwater drilling riser systems via delayed H_∞ control. *ISA Trans*, 133:248-261. https://doi.org/10.1016/j.isatra.2022.07.003

Zhang XM, Han QL, Ge XH, et al., 2020. Networked control systems: a survey of trends and techniques. *IEEE/CAA J Autom Sin*, 7(1):1-17. https://doi.org/10.1109/JAS.2019.1911651

Zhang XM, Han QL, Ge XH, 2022. A novel approach to H_∞ performance analysis of discrete-time networked systems subject to network-induced delays and malicious packet dropouts. *Automatica*, 136:110010. https://doi.org/10.1016/j.automatica.2021.110010

Zhang XM, Han QL, Ge XH, et al., 2023. Sampled-data control systems with non-uniform sampling: a survey of methods and trends. *Annu Rev Contr*, 55:70-91. https://doi.org/10.1016/j.arcontrol.2023.03.004

Zhao YD, Sun YT, Zhang BL, et al., 2022a. Delay-feedback-based recoil control for deepwater drilling riser systems. *Int J Syst Sci*, 53(12):2535-2548. https://doi.org/10.1080/00207721.2022.2063966

Zhao YD, Sun YT, Zhang BL, et al., 2022b. Recoil control of deepwater drilling riser systems via optimal control with feedforward mechanisms. *Ocean Eng*, 257:111690. https://doi.org/10.1016/j.oceaneng.2022.111690

Zou L, Wang ZD, Gao HJ, 2016. Observer-based H_∞ control of networked systems with stochastic communication protocol: the finite-horizon case. *Automatica*, 63:366-373. https://doi.org/10.1016/j.automatica.2015.10.045

List of supplementary materials

1 Proof of Theorem 1

2 Proof of Theorem 2